Table 1
The Primers used to amplify *YWHAE*.

Exon	Forward primer	Reverse primer	Annealing Tm (C°)	PCR product
1-1	5′-CTTGGCCGAGAAAACTAGG-3′	5′-GGGACTGCTCCTGAAAAA-3′	56	491
1-2	5′-AGTGACAGCCTCAGATTTCG-3′	5′-ATCCTCTCGATCATCCAT-3′	54	497
1-3	5′-CCATGACAGAAACCGTTACA-3′	5′-GCCATTTTACAACCAACTCC-3′	54	775
2	5′-TGGCTCTTAGTTTGGTTTCC-3′	5′-TTTGTCCTCATGCATAG-3′	54	577
3	5′-GAAGGAAGAAGGGAGTTTGG-3′	5′-CTGTGAAATGTATGCCGTTT-3′	54	493
4	5′-AAAATGAAACGAAGCCAGTT-3′	5′-TGGAACTCCGTACTGTAGCA-3′	54	488
5	5′-GAAGAAAAGATTGCTGTCTAGC-3′	5′-TGGAACTCCGTACTGTAGCA-3′	56	398
6	5′-AGAGTCTTTATGCTTGGAATGA-3′	5′-AGTGTCTTAAAGAACCTAAAAGC-3′	54	387

containing either the human *YWHAE* promoter (−469/−449) with the wild type C/EBP enhancer element (shown underlined, 5′-TCA GAT TTC GGG AAA GAA GAC-3′), or the human *YWHAE* promoter (−469/−449) with the mutated C/EBP sequence (shown underlined, 5′-TCA GAT TTC GGT AAA GAA GAC-3′), and 4% beaded-agarose conjugated with streptavidin. The beads were collected by centrifugation. Nuclear proteins bound to the beads were dissociated and analyzed by Western blotting. The following antibody was used: C/EBPβ (Santa Cruz, sc-150, 1:200).

2.7. Western blotting

E18.5 embryo hearts were harvested and snap-frozen in liquid nitrogen and stored at −80 °C. Hearts were processed in RIPA buffer containing 1× complete, EDTA-free Protease Inhibitors Cocktail (Roche Applied Science, 04693132001). Protein concentration was determined using Pierce® BCA Protein Assay Kit (Thermo Scientific, 23225). Western blotting was performed by a procedure described previously (Brunelli, et al., 2007). Briefly, 30 or 50 μg protein was separated on 4–15% or 8–16% gradient SDS-polyacrylamide gels and electroblotted on nitrocellulose membranes, blocked with 5% milk, followed by incubation with the following primary antibody at the indicated dilutions: C/EBPβ (Santa Cruz, sc-150, 1:200). After appropriate washing of unspecific antibody binding, secondary peroxidase-conjugated antibody was applied. To detect signal, membranes were incubated with an ECL chemiluminescence detection system (Pierce).

2.8. Statistical analysis

Student's *t*-test software (Smith's Statistical Package, at http://www.economics. pomona.edu/StatSite/framepg.html) was used to determine statistical differences of promoter analyses. A p value of <0.05 was considered statistically significant.

3. Results

3.1. Molecular analysis

Seven novel variants were identified in this patient cohort (Table 2 and Fig. 1). Four of these variants were located within the promoter, one was intronic, one was a synonymous substitution in exon 6 and the last was in the 3′ untranslated region. None of the variants were predicted to alter RNA splicing or exonic splice enhancer (ESE) sequences by multiple *in silico* analyses (http://www.fruitfly.org/seq_tools/splice.html, http://genes.mit.edu/exonscan/, http://genes.mit.edu/burgelab/rescue-ese/, and http://www.cbs.dtu.dk/services/NetGene2/). Five of the variants were identified in the control samples at frequencies statistically indistinguishable from the patient cohort. Of the two variants that were not detected in the control cohort, one (c.−458 G>T) is located in a consensus C/EBP response element of the promoter (Fig. 2A) while the other (c.64+9G>A) was not predicted to alter mRNA splicing. The promoter variant was identified in a familial patient who was negative for mutations in the following LVNC associated genes: *TAZ, DTNA, LDB3, FKBP12, STN, CSX/Nkx2.5* and *SCN5A*.

Table 2
Variants identified in *YWHAE* in LVNC patients.

Location	DNA variant	Protein change	Frequency in Patients	Frequency in Controls
Promoter	c.−798C>T	NA	10/77(5F/5S)	14/200
Promoter	c.−751insG	NA	5/77(2F/3S)	9/200
Promoter	c. −458G>T	NA	1/77(1F)	0/200
Promoter	c.−54G>C	NA	11/77(5F/6S)	17/200
Intron 1	c.64+9G>A	NA	1/77(S)	0/200
Exon 6	c.756C>T	p.Asp252=	1/77(S)	1/100
3′ UTR	c.823C>T	NA	2/77(2S)	1/100

NA: Not applicable; F: Familial; S: Sporadic.

3.2. Functional analysis of the promoter variant

In order to investigate the effect of the −458G>T variant on promoter activity, we generated constructs with the promoter (wild type and mutant) driving the expression of firefly luciferase. Expression of these constructs in human ECV-304 cells revealed that the activity of the mutant promoter was decreased by at least 50% compared to the wild type promoter (Fig. 2B). Using *in silico* analysis, we found that −458G>T generates a *bona fide* C/EBP consensus sequence at −463/−456 (TTCGGGAA to TTCGGTAA), predicting increased affinity for the three C/EBPβ isoforms: full-length liver-activating protein (LAP*), medium-length liver-activating protein (LAP) and liver-inhibitory protein (LIP). Based on this information, we performed *in vitro* DNA binding studies. Compared to a wild type probe, the −458G>T mutant probe increased binding of LAP* and LIP, while binding of LAP was only modestly increased (Fig. 2C, panels a and b). As the role of C/EBPβ in the heart is not well known, we measured its expression, and confirmed that C/EBPβ is robustly expressed in the mouse heart, with LAP* being the most abundant isoform (Fig. 2D). Overall, these data suggest that increased binding of C/EBP inhibitory isoforms accounts for decreased activity of the −458G>T variant in the 14-3-3ε promoter.

3.3. Clinical characteristics of the patients with the −458 G>T variant

The −458G>T promoter variant was identified in a kindred in which there is significant family history of LVNC and/or sudden death in early childhood and the pedigree structure indicates autosomal dominant inheritance (Fig. 3) since there appears to be male to male transmission, which would exclude X-linked inheritance. However, there are multiple intermarriages and this could confound this interpretation. The proband (Fig. 3, V-3) was screened just after birth because of the family history of multiple early infant deaths due to heart failure. He was found to have LV noncompaction on echocardiography. His elder brothers (V-1 and V-2) died because of severe heart failure at 2 weeks and 9 months of age, respectively. Echocardiography at 5 months of age revealed a thick noncompacted layer and thin compacted layer in the apex of the left ventricle and slightly depressed LV function (LVDd = 23.8 mm, EF = 63%) (Fig. 4A). He had coarse facial appearance and cataracts, severe growth retardation and developmental delay since

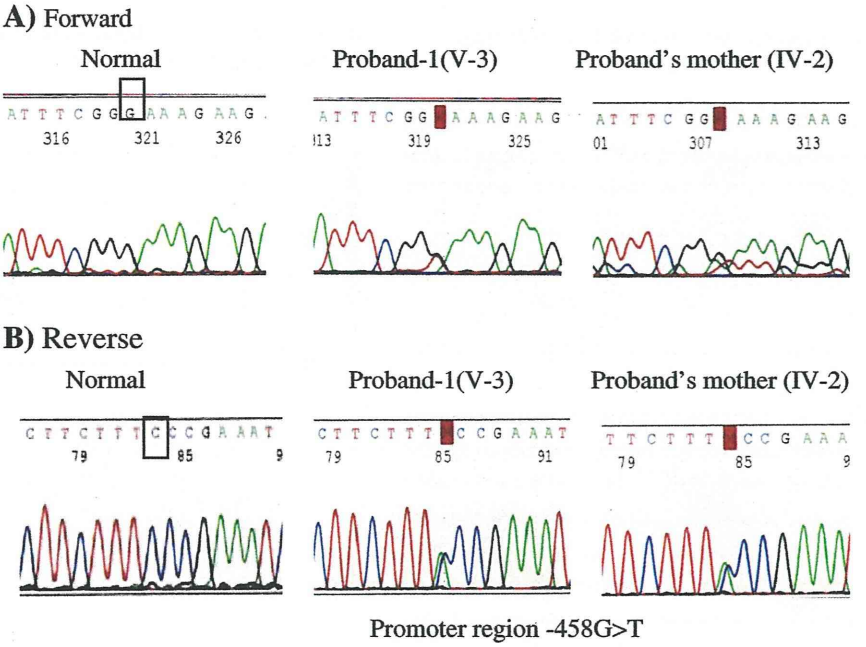

Fig. 1. DNA sequence electropherograms showing identification of the heterozygous c. −458G>T substitution using forward (panel A) and reverse (panel B) primers in the proband.

birth. His brain MR images both at 1 month and 5 months of age showed hypoplasia of the corpus callosum, and at 4 years of age profound brain atrophy in both the white and gray matters (Fig. 4B). He died suddenly because of intractable heart failure at 5 years of age. The proband and his second brother were noted to have 3-methylglutaconic aciduria, but did not have neutropenia typical of Barth syndrome. In addition, analysis of *TAZ* did not identify variants. The mother of the proband carried the same *YWHAE* variant. She remains asymptomatic but has two brothers who died prematurely, both at 3 years of age, from presumed heart failure. DNA was not available from any other family member.

4. Discussion

LVNC is a human cardiomyopathy originating from an arrest of normal ventricular morphogenesis, but the genes controlling this key developmental process remain poorly understood. *TAZ* is one of candidate genes for LVNC, and allelic with Barth syndrome. Barth syndrome is associated with a variety of clinical features including cardiomyopathy, skeletal myopathy, neutropenia, growth delay, normal cognitive function and 3-methylglutaconic aciduria. The proband and an affected brother had elevated 3-methylglutaconic acid and LVNC suggesting Barth syndrome. We previously reported *TAZ* mutations in 3 probands and their families (Chang et al., 2010; Chen et al., 2002; Xing et al., 2006), however we could not find any mutation in this proband. While direct DNA sequencing can identify single nucleotide variations and small exonic insertions–deletions (indels), there could be large intronic indels or gene rearrangements that were not detected using this approach. In addition, there are several instances of apparent male to male transmission in this family (Fig. 3), which would exclude an X-linked mode of inheritance. However, the consanguinity present in this family means that this mode of inheritance is also possible. Although we could not definitively exclude the diagnosis of Barth syndrome, the patient carrying the *YWHAE* promoter variant has other distinctive clinical findings. Brain malformation and severe developmental delay, which were seen in our patient, are distinct findings from Barth syndrome, and have not been reported as part of the syndrome. *TAZ* itself is not engaged in neural development. Other clinical findings of coarse facial appearance with cataracts, prominent forehead, and saddle nose, and severe motor delay since birth do not match the typical features of Barth syndrome. Thus, we believed that the clinical phenotype of this proband was different from the Barth syndrome, and we looked for another candidate or additional genes. In addition, 3-methylglutaconic aciduria is found not only in Barth syndrome but also in other disorders of the oxidative phosphorylation, including type 1 (inborn error of leucine catabolism), type 2 (Barth syndrome), type 3 (Costeff syndrome), and type 4 (unspecified), possibly similar to this proband. 14-3-3ε, encoded by *YWHAE*, has been shown to play important roles in neuronal development, and is involved in Miller–Dieker syndrome, a lissencephaly syndrome. We recently showed that mice lacking this gene develop LVNC (Kosaka et al., in press). Therefore, we hypothesized that variants in *YWHAE* may contribute to the pathophysiology of LVNC with brain malformation in this patient.

In this study, we identified a novel variant of *YWHAE* (14-3-3ε protein) in a patient with LVNC and hypoplasia of the corpus callosum. This variant (c.−458G>T) is located in a regulatory C/EBP response element, and was shown to result in a significant reduction in *YWHAE* promoter activity, possibly accounting, at least in part, for the LVNC phenotype of the patient. Interestingly, heterozygous loss of *YWHAE* has been linked to cerebral anomalies similar to the ones reported in our LVNC patient, and numerous LVNC patients with neuromuscular disease have been described in the literature (Mignon-Ravix et al., 2010; Schiff et al., 2010; Stollberger et al., 2002). Furthermore, we recently showed that 14-3-3ε has a dose–responsive role in ventricular morphogenesis, and our previous data show that C/EBPβ is a key regulator of *YWHAE* expression (Brunelli et al., 2007). Our data are in agreement with the hypothesis that human LVNC results from an arrest of normal ventricular morphogenesis because they suggest a model in which decreased proliferation of compact myocardium with preservation of trabecular myocardium growth leads to a relative overrepresentation of the trabeculae at birth, consistent with a histologic diagnosis of noncompaction (Kosaka et al., in press).

The variant did not abrogate completely *YWHAE* promoter activity and our analysis was performed *in vitro*. However, repression may

A) Nucleotide Sequence of the Human *YWHAE* Promoter Region

```
-1524  CCCTCATCTA ACAAATTCCC TGCTCCTATT CATAGTGGGC CTAGGGAGGG
-1474  AAAAAGGTTA AACAGGAGAA GACAAAGATC AGTGTGAGGG GAAAGTTGAG
            PPAR          PPAR          PPAR
-1424  GCGTGAAAAC TGGAGCTCCC CTGTCCCTGA CAACTGTAAC AGGGCCCAGT
.....  .....................  .....................  .....................  .....................  .....................
.....  .....................  .....................  .....................  .....................  .....................
.....  .....................  .....................  .....................  .....................  .....................
-624   CAGCAGAATC ACTTGAACCC GGGAAGGCGG ACGTTGTGGT AACCCGAGAT
                              SP1          C/EBP
-574   CGCACCACTG CACTCCAGCC TGGGGAACAA GAGGGAAACT CCGTCTCAAA
                                        NF-κB
-524   AAGAAAAAAG AAAAAAGAAA AAAGAAAAGA AAACCAGGGC GCGGTAGTGA
-474   CAGCCTCAGA TTTCGGGAAA GAAGACCTGC CATGACAGAA ACCGTTACAG
            C/EBP
-424   CCTCCGTCGT TCTTTTCCGC AGGTCGGGCC TCGGGCCCCG GTCTGACCCA
-374   GGTCTCTCGC TGGCTTTTTT CAGGAGCAGT CCCGGCCGGC CCCGCCTCAG
                                  NF-κB          SP1
-324   CCCTTCTCGT TCCCCGGGGG CCGCTCCCTT TCGGCAGTCG CAGTTCCCGC
                              NF-κB
-274   CTCTGGGCTC CGGCGCCCGC TGAGCCGACA GAGGAGAGGC GTCTCGTGCG
-224   CTCGTTCCAG CCGCTTCGGG CGCCGAGTTC CAGGACCCGC CCCCCGCGCC
                                                 SP1
-174   AGTTGCCAGG GAGCGGTTGC CATAGAGCTG AGCAGTTGTC CGCGTGCGCA
                     C/EBP
-124   GGCGGAAGTC CCGGATTGAG GCGCCGCCAT TTTTGCTGCC CGGACGCGGA
            NF-κB      *
```

B) The -458G>T *YWHAE* Variant Leads to Decreased Promoter Activity

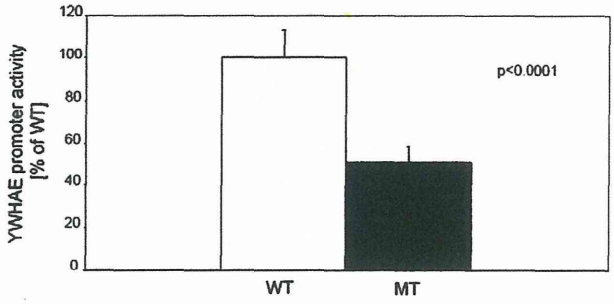

C) The -458G>T Variant Increases Binding of the C/EBPβ Isoforms LAP* and LIP

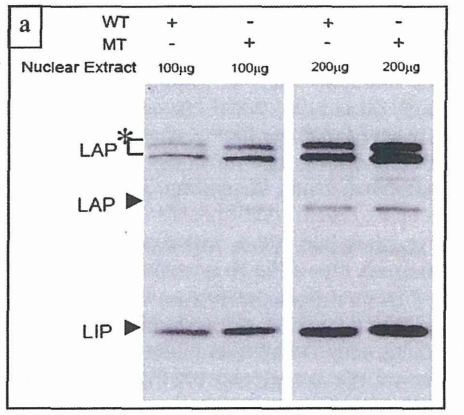

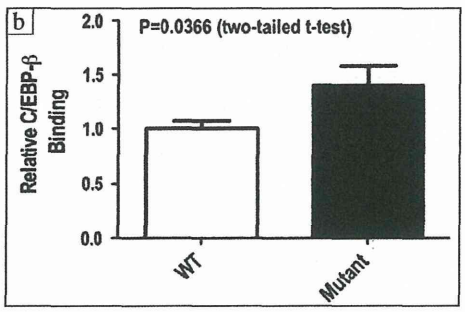

D) Expression of C/EBPβ isoforms in E18.5 mouse hearts

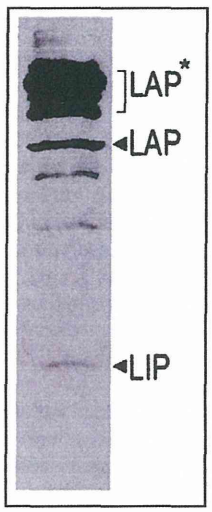

Fig. 2. Functional analysis of the *YWHAE* promoter variant. A. Nucleotide sequence of the human *YWHAE* promoter region. Numbers are relative to the translation start site ATG (not shown). Multiple C/EBP response elements are present and the −466/−453 binding site carrying the −458G>T point mutation is identified by the boxed G. The asterisk indicates the major transcription start site (adapted from Reijnen et al. (1992). B. The −458G>T variant decreases *YWHAE* promoter activity. ECV-304 cells were transfected with either a wild type or a mutant promoter carrying the −458G>T variant; then the promoter activity was measured. The activity of the mutant promoter was 50% compared to the wild type control ($p<0.0001$, Student's *t*-test). WT = wild type promoter construct. MT = promoter construct containing the −458G>T point mutation. C. The −458G>T *YWHAE* promoter variant increases binding of the C/EBPβ isoforms LAP* and LIP (panels a and b). (a) Nuclear proteins were collected from ECV-304 cells and C/EBPβ binding to a wild type (TTCGGGAAA) or mutant type (TTCGGTAAA) probe containing the specific −463/−456 C/EBPβ response element of *YWHAE* was determined by streptavidin pull down binding assay as described under "Materials and methods". Increased binding of LAP* to the mutant probe was evident at both concentrations of nuclear proteins (100 μg and 200 μg). All lanes belong to the same gel. (b) C/EBPβ binding for the −458G>T variant and wild type promoter was quantified. In three independent experiments, the mean densitometry (expressed in arbitrary units) was calculated, and the densitometry of the mutant promoter was expressed relative to the wild type promoter. WT = wild type probe. MT = probe containing the −458G>T point mutation. D. Expression of C/EBPβ isoforms in E18.5 mouse hearts. All three C/EBPβ isoforms, LAP*, LAP, and LIP are expressed in the heart, but LAP* is the most abundant. There are two aspecific bands between LAP and LIP.

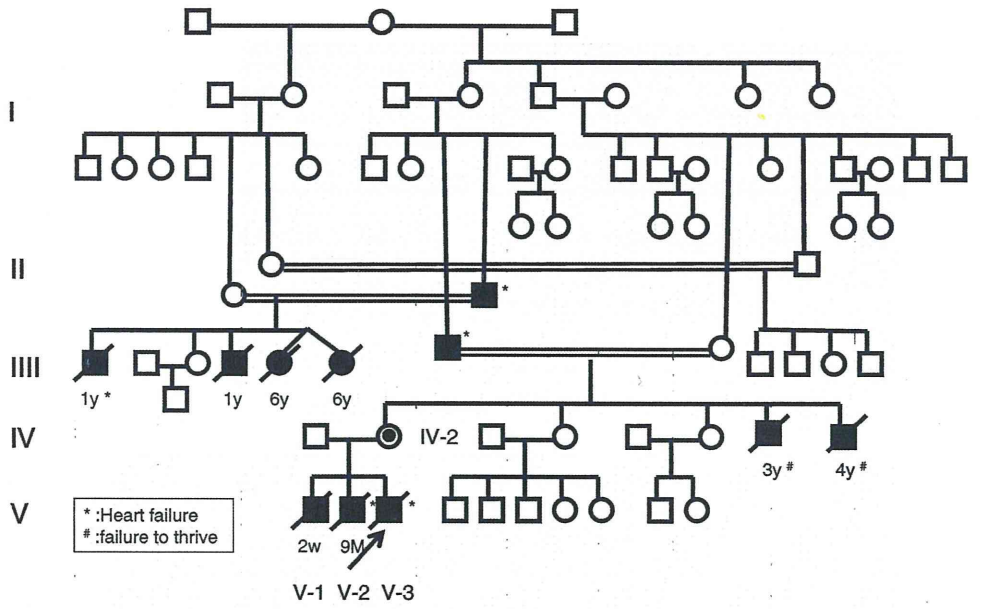

Fig. 3. The pedigree of the family of the proband. The proband is indicated by an arrow. There multiple infant deaths, both of males and females. The patient and his two elder brothers died due to severe heart failure at 5 years, 2 weeks and 9 months of age, respectively. Although there are many intermarriages in this family, the phenotype of the proband and siblings suggests an autosomal dominant inheritance.

change depending on the level of specific *trans*-activators and the chromatin environment, and previous investigations used *in vitro* analysis to identify point mutations that depress promoter activity, causing diseases such as β thalassemia, pyruvate kinase deficiency, and hemophilia B (Crossley and Brownlee, 1990; Kulozik et al., 1991; Ludlow et al., 1996; Reijnen et al., 1992; van Wijk et al., 2003). Importantly, we previously established, using the same cell line of this study, that *in vitro* analysis of the *YWHAE* promoter provides an accurate estimate of *in vivo* binding of *trans*-acting factors and that *YWHAE* promoter activity provides a precise estimate of *YWHAE* mRNA and 14-3-3ε protein level (Brunelli et al., 2007). We used a human endothelial cell line for our analysis because, to our knowledge, human ventricular cardiomyocyte lines are not available (Kosaka et al., in press). Taken together, these data provide evidence that the *YWHAE* −458G>T variant may be involved in human LVNC.

14-3-3 proteins modulate crucial aspects of heart function both *in vitro* and *in vivo* (Allouis et al., 2006; Choe et al., 2006; Kagan et al., 2002; Zhang et al., 2003). Notably, 14-3-3 proteins were the first molecules identified as discrete binding partners of phosphoserine/threonine (pSer/Thr) residues in proteins, recognizing the sequence RSXpSXP or RXXXpSXP (Muslin et al., 1996; Yaffe et al., 1997). This explains their critical role in signal transduction because 14-3-3 proteins modulate the recruitment of pSer/Thr-containing proteins into larger signaling complexes. Mice lacking one or both copies of *Ywhae* have a cardiac phenotype characteristic of LVNC, as well as VSDs (Kosaka et al., in press), suggesting that decreased levels of 14-3-3ε can be involved in abnormal cardiac morphogenesis. However, other factors are clearly involved in our proband because his mother did not have evidence of cardiac disease despite carrying the −458G>T *YWHAE* variant. Interestingly, the variant appears to increase binding of the C/EBPβ isoform LAP*. The role of C/EBPβ in the heart is incompletely understood, but it is expressed during cardiogenesis (Kousteni et al., 1998), in proliferating cardiomyocytes, as well as in the adult heart (Cao et al., 1991), and has recently been involved in regulating cardiomyocyte hypertrophy and proliferation (Bostrom et al., 2010). Furthermore, we have shown that C/EBPβ is a key regulator of *YWHAE* expression (Brunelli et al., 2007). It remains unclear which C/EBP isoforms account for the inhibitory effect on the −458G>T *YWHAE* variant. LIP has classically been considered an inhibitory isoform. Contrary to the common belief that LAP* functions only as a transactivator, some studies have shown that LAP* can be an inhibitor, such as downregulating *CCND1* (Eaton and Sealy, 2003; Eaton et al., 2001). Therefore, we suggest that increased binding of both LIP and LAP* contributes to the inhibition of the −458G>T *YWHAE* variant. In addition, our data imply that C/EBPβ plays important roles in the heart, particularly in LVNC.

It was previously reported that *Ywhae* haploinsufficiency in mice leads to brain malformations (Toyo-oka et al., 2003). Further, Miller–Dieker syndrome (or 17p13.3 deletion syndrome) is characterized by lissencephaly, mental retardation and facial dysmorphism. This region of chromosome 17p13 encodes *YWHAE* and *PAFAH1B1*, and recently Schiff et al. showed that patients lacking only *YWHAE* have phenotypes that include mild mental retardation, moderate to severe growth restriction, white matter abnormalities and developmental defects (Kulozik et al., 1991). In addition, a small deletion of 17p13.3 encompassing *YWHAE* was described in a patient presenting with periventricular nodular heterotopias and marked corpus callosum hypoplasia (Mignon-Ravix et al., 2010). This phenotype could represent the human counterpart of the abnormal cortical organization phenotype identified in *Ywhae* heterozygous knock-out mice (Toyo-oka et al., 2003). However, no information on cardiac structure or function was provided in this case, and we are not aware of any echocardiographic studies being consistently performed in patients with Miller–Dieker syndrome although some have structural cardiac defects, such as atrial septal defects. Interestingly, our proband carrying the c.−458>T variant suffered severe developmental delay, as well as facial and optical abnormalities. His brain MRI and CT showed hypoplasia of the corpus callosum from an early stage of life, and later profound brain atrophy in white matter and gray matter. However, heterotopia or pachygyria was not detected on his brain MRI, changes seen in patients with 17p13.3 deletion syndrome (Kato and Dobyns, 2003). Regardless, our data suggest that this variant, resulting in a significant decrease in *YWHAE* expression, may be sufficient to recapitulate many of the effects of the deletion of 17p13.3.

These data are consistent with our recent data showing that mice with 14-3-3ε deletion present evidence of ventricular noncompaction (Kosaka et al., in press), and suggest that *YWHAE* is a novel candidate

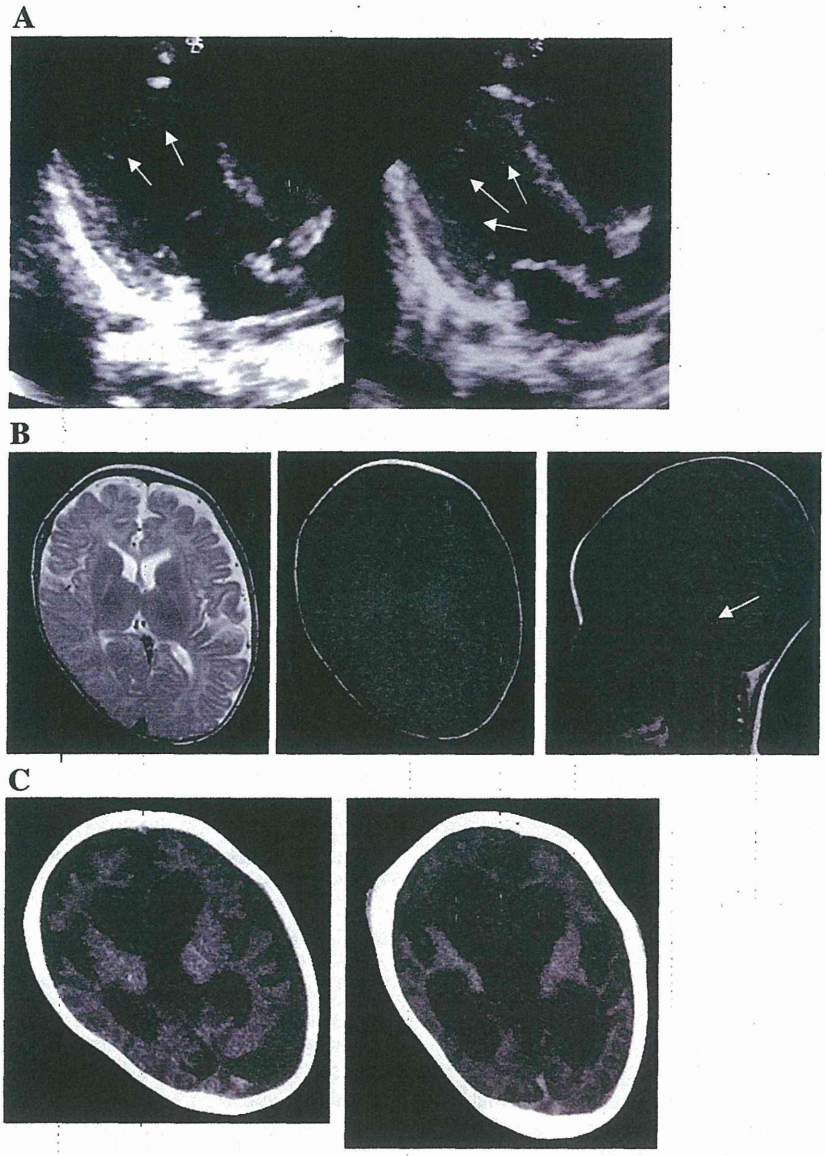

Fig. 4. A. Echocardiography of the proband at 5 months of age revealed thick noncompacted layer (white arrows) and thin compacted layer in the apex of the left ventricle and slightly depressed LV function (LVDd = 23.8 mm, EF = 63%). Long axis view of the left ventricle in diastole (left) and systole (right). B. Brain MRI of the proband at 5 months of age. Left: axial T2 weighted image; middle: axial T1 weighted image; right: sagittal T1 weighted image showing mild cortical atrophy and pronounced hypoplasia of the corpus callosum (white arrow). C. Brain CT of the proband at 4 (left) and 5 (right) years of age showing severe brain atrophy both in the white and gray matters.

gene for LVNC, and should especially be considered in patients with otherwise unexplained developmental delay, as well as facial and optical abnormalities.

Acknowledgments

The authors wish to acknowledge noncompaction study collaborators: Tadaro Abe, Yo Arita, Hikaru Doi, Yutaka Fukuda, Norihide Fukushima, Taketoshi Hayakawa, Tamaki Hayashi, Takashi Higaki, Yoshimi Hiraumi, Hitoshi Horigome, Yumiko Ikemoto, Takehiko Ishida, Astuko Ishihara, Shiro Ishikawa, Takamitsu Ishikawa, Satoru Iwashima, Hiromi Katayama, Shinji Kaichi, Hiroki Kajino, Tohru Kubo, Atsushi Kuwabara, Kyoko Sekiguchi,Naomasa Makita, Hiroshi Mito, Toshihiro Mitomori, Hiroyuki Matsuura, Masaru Miura, Kazuhiro Mori, Yasuhiro Morikami, Yasuo Murakami, Masao Nakagawa, Koji Nakamura, Tomotaka Nakayama, Koichi Nihei, Masaki Nii, Yuichi Nomura, Junichi Ohata, Yoko Okada, Shin Ono, Hiroo Ooki, Mitsuo Takeda, Satoshi Takenaka, Masamichi Tamura, Yasuhiko Tanaka, Kazuhiro Terano, Mika Tokuyama, Hideshi Tomita, Masaki Tsukashita, Takara Tsumori, Takashi Urashima, Yasunobu Wakabayashi, Masaki Yamamoto, Kenji Yasuda, Muneo Yoshibayashi, Jun Yoshimoto and Hiroyuki Yoshizawa.

The authors sincerely thank Tatsujiro Oka for his help. The authors wish to acknowledge Yoshiko Ohnuma, Hitoshi Moriuchi and Chikako Sakai for their expert technical assistance. We are also grateful to Dr. Nikolaj A. Timchenko for providing the LAP*, LAP and LIP C/EBPβ plasmids. Fukiko Ichida was supported by grants from the Ministry of Education, Culture, Sports, Science and Technology in Japan (Grant-in-Aid for scientific Research Grant-in-Aid for Scientific Research No.17591072, No.20591274). Luca Brunelli was supported by an American Heart Association, Beginning Grant-In-Aid, Western States Affiliate.

Disclosure statement

None.

References

Aitken, A., et al., 1992. 14-3-3 proteins: a highly conserved, widespread family of eukaryotic proteins. Trends Biochem. Sci. 17, 498–501.

Allouis, M., et al., 2006. 14-3-3 is a regulator of the cardiac voltage-gated sodium channel nav1.5. Circ. Res. 98, 1538–1546.

Bartram, U., Bauer, J., Schranz, D., 2007. Primary noncompaction of the ventricular myocardium from the morphogenetic standpoint. Pediatr. Cardiol. 28, 325–332.

Bostrom, P., et al., 2010. C/ebpbeta controls exercise-induced cardiac growth and protects against pathological cardiac remodeling. Cell 14, 1072–1083.

Brunelli, L., Cieslik, K.A., Alcorn, J.L., Vatta, M., Baldini, A., 2007. Peroisome proliferator-activated receptor-delta upregulates 14-3-3 epsilon in human endothelial cells *via* ccaat/enhancer binding protein-beta. Circ. Res. 100, e59–e71.

Cao, Z., Umek, R.M., McKnight, S.L., 1991. Regulated expression of three c/ebp isoforms during adipose conversion of 3t3-l1 cells. Genes Dev. 5, 1538–1552.

Chang, B., et al., 2010. Noncompaction study collaborators Gonadal mosaicism of a TAZ (G4.5) mutation in a Japanese family with Barth syndrome and left ventricular noncompaction. Mol. Genet. Metab. 100, 198–203.

Chen, R., et al., 2002. Mutation analysis of the g4.5 gene in patients with isolated left ventricular noncompaction. Mol. Genet. Metab. 77, 319–325.

Chin, T.K., Perloff, J.K., Williams, R.G., Jue, K., Mohrmann, R., 1990. Isolated noncompaction of left ventricular myocardium. A study of eight cases. Circulation 82, 507–513.

Choe, C.U., et al., 2006. C-terminal herg (lqt2) mutations disrupt ikr channel regulation through 14-3-3epsilon. Hum. Mol. Genet. 15, 2888–2902.

Crossley, M., Brownlee, G.G., 1990. Disruption of a c/ebp binding site in the factor ix promoter is associated with haemophilia b. Nature 345, 444–446.

Dusek, J., Ostadal, B., Duskova, M., 1975. Postnatal persistence of spongy myocardium with embryonic blood supply. Arch. Pathol. 99, 312–317.

Eaton, E.M., Sealy, L., 2003. Modification of ccaat/enhancer-binding protein-beta by the small ubiquitin-like modifier (sumo) family members, sumo-2 and sumo-3. J. Biol. Chem. 278, 33416–33421.

Eaton, E.M., Hanlon, M., Bundy, L., Sealy, L., 2001. Characterization of c/ebpbeta isoforms in normal *versus* neoplastic mammary epithelial cells. J. Cell. Physiol. 189, 91–105.

Fu, H., Subramanian, R.R., Masters, S.C., 2006. 14-3-3 proteins: structure, function, and regulation. Annu. Rev. Pharmacol. Toxicol. 40, 617–647.

Han, D.C., Rodriguez, L.G., Guan, J.L., 2001. Identification of a novel interaction between integrin beta1 and 14-3-3beta. Oncogene 20, 346–357.

Hermida-Prieto, M., et al., 2004. Familial dilated cardiomyopathy and isolated left ventricular noncompaction associated with lamin a/c gene mutations. Am. J. Cardiol. 94, 50–54.

Ichida, F., et al., 1999. Clinical features of isolated noncompaction of the ventricular myocardium: long-term clinical course, hemodynamic properties, and genetic background. J. Am. Coll. Cardiol. 34, 233–240.

Ichida, F., et al., 2001. Novel gene mutations in patients with left ventricular noncompaction or barth syndrome. Circulation 103, 1256–1263.

Jenni, R., Rojas, J., Oechslin, E., 1999. Isolated noncompaction of the myocardium. N. Engl. J. Med. 340, 966–967.

Jenni, R., Oechslin, E.N., van der Loo, B., 2007. Isolated ventricular non-compaction of the myocardium in adults. Heart 93, 11–15.

Kagan, A., Melman, Y.F., Krumerman, A., McDonald, T.V., 2002. 14-3-3 amplifies and prolongs adrenergic stimulation of herg k+ channel activity. EMBO J. 21, 1889–1898.

Kato, M., Dobyns, W.B., 2003. Lissencephaly and the molecular basis of neuronal migration. Hum. Mol. Genet. R89–R96 (12 Spec No 1).

Klaassen, S., et al., 2008. Mutations in sarcomere protein genes in left ventricular noncompaction. Circulation 117, 2893–2901.

Kosaka, Y., Cieslik, K.A., Li, L., Lezin, G., Maguire, C.T., Saijoh, Y., Toyo-oka, K., Gambello, M.J., Vatta, M., Wynshaw-Boris, A., Baldini, A., Yost, H.J., Brunelli, L., in press. 14-3-3 e plays a role in cardiac ventricular compaction by regulating the cardiomyocyte cell cycle. Mol. Cell. Biol.

Kousteni, S., Kockar, F.T., Sweeney, G.E., Ramji, D.P., 1998. Characterisation and developmental regulation of the xenopus laevis ccaat-enhancer binding protein beta gene. Mech. Dev. 77, 143–148.

Kulozik, A.E., Bellan-Koch, A., Bail, S., Kohne, E., Kleihauer, E., 1991. Thalassemia intermedia: moderate reduction of beta globin gene transcriptional activity by a novel mutation of the proximal caccc promoter element. Blood 77, 2054–2058.

Ludlow, L.B., et al., 1996. Identification of a mutation in a gata binding site of the platelet glycoprotein ibbeta promoter resulting in the Bernard–Soulier syndrome. J. Biol. Chem. 271, 22076–22080.

Maron, B.J., et al., 2006. Contemporary definitions and classification of the cardiomyopathies: an American Heart Association Scientific Statement From the Council on Clinical Cardiology, Heart Failure and Transplantation Committee; quality of care and outcomes research and functional genomics and translational biology interdisciplinary working groups; and council on epidemiology and prevention. Circulation 113, 1807–1816.

Mignon-Ravix, C., et al., 2010. Deletion of ywhae in a patient with periventricular heterotopias and pronounced corpus callosum hypoplasia. J. Med. Genet. 47, 132–136.

Muslin, A.J., Tanner, J.W., Allen, P.M., Shaw, A.S., 1996. Interaction of 14-3-3 with signaling proteins is mediated by the recognition of phosphoserine. Cell 84, 889–897.

Oechslin, E.N., Attenhofer Jost, C.H., Rojas, J.R., Kaufmann, P.A., Jenni, R., 2000. Long-term follow-up of 34 adults with isolated left ventricular noncompaction: a distinct cardiomyopathy with poor prognosis. J. Am. Coll. Cardiol. 36, 493–500.

Pignatelli, R.H., et al., 2003. Clinical characterization of left ventricular noncompaction in children: a relatively common form of cardiomyopathy. Circulation 108, 2672–2678.

Reijnen, M.J., Sladek, F.M., Bertina, R.M., Reitsma, P.H., 1992. Disruption of a binding site for hepatocyte nuclear factor 4 results in hemophilia b leyden. Proc. Natl. Acad. Sci. U. S. A. 89, 6300–6303.

Ritter, M., Oechslin, E., Sutsch, G., Attenhofer, C., Schneider, J., Jenni, R., 1997. Isolated noncompaction of the myocardium in adults. Mayo Clin. Proc. 72, 26–31.

Sasse-Klaassen, S., Gerull, B., Oechslin, E., Jenni, R., Thierfelder, L., 2003. Isolated noncompaction of the left ventricular myocardium in the adult is an autosomal dominant disorder in the majority of patients. Am. J. Med. Genet. A 119A, 162–167.

Schiff, M., et al., 2010. Further delineation of the 17p13.3 microdeletion involving ywhae but distal to pafah1b1: four additional patients. Eur. J. Med. Genet. 53, 303–308.

Shan, L., et al., 2008. SCN5A variants in japanese patients with left ventricular noncompaction and arrhythmia. Mol. Genet. Metab. 93, 468–474.

Stollberger, C., Finsterer, J., Blazek, G., 2002. Left ventricular hypertrabeculation/noncompaction and association with additional cardiac abnormalities and neuromuscular disorders. Am. J. Cardiol. 90, 899–902.

Toyo-oka, K., et al., 2003. 14-3-3epsilon is important for neuronal migration by binding to nudel: a molecular explanation for miller-dieker syndrome. Nat. Genet. 34, 274–285.

Tzivion, G., Shen, Y.H., Zhu, J., 2001. 14-3-3 proteins; bringing new definitions to scaffolding. Oncogene 20, 6331–6338.

van Wijk, R., et al., 2003. Disruption of a novel regulatory element in the erythroid-specific promoter of the human pklr gene causes severe pyruvate kinase deficiency. Blood 101, 1596–1602.

Vatta, M., et al., 2003. Mutations in cypher/zasp in patients with dilated cardiomyopathy and left ventricular non-compaction. J. Am. Coll. Cardiol. 42, 2014–2027.

Wilker, E., Yaffe, M.B., 2004. 14-3-3 proteins—a focus on cancer and human disease. J. Mol. Cell. Cardiol. 37, 633–642.

Xing, Y., et al., 2006. Genetic analysis in patients with left ventricular noncompaction and evidence for genetic heterogeneity. Mol. Genet. Metab. 88, 71–77.

Yaffe, M.B., et al., 1997. The structural basis for 14-3-3: phosphopeptide binding specificity. Cell 91 (-971).

Zhang, S., Ren, J., Zhang, C.E., Treskov, I., Wang, Y., Muslin, A.J., 2003. Role of 14-3-3-mediated p38 mitogen-activated protein kinase inhibition in cardiac myocyte survival. Circ. Res. 93, 1026–1028.

Gene 517 (2013) 125–127

Contents lists available at SciVerse ScienceDirect

Gene

journal homepage: www.elsevier.com/locate/gene

Short Communication

A novel homozygous *GALC* mutation: Very early onset and rapidly progressive Krabbe disease

Fatih Kardas [a], Asli Subasioglu Uzak [b,*], Mohammad Arif Hossain [c], Norio Sakai [c], Mehmet Canpolat [d], Ali Yıkılmaz [e]

[a] Department of Pediatric Nutrition and Metabolism, Erciyes University School of Medicine, Kayseri, 38039, Turkey
[b] Department of Medical Genetics, Erciyes University School of Medicine, Kayseri, 38039, Turkey
[c] Department of Pediatrics, Osaka University Graduate School of Medicine, 2-2 Yamada-oka, Suita, Osaka 565-0871, Japan
[d] Department of Pediatric Neurology, Erciyes University School of Medicine, Kayseri, 38039, Turkey
[e] Department of Pediatric Radiology, Erciyes University School of Medicine, Kayseri, 38039, Turkey

ARTICLE INFO

Article history:
Accepted 2 December 2012
Available online 28 December 2012

Keywords:
Krabbe disease
GALC gene
Galactocerebrosidase

ABSTRACT

A clear cut genotype–phenotype correlation for Krabbe disease is not available. Therefore, it is important to identify new mutations and their associated phenotypes to predict the prognosis of the disease. The aim of this study is to identify the causative mutation(s) in a family with Krabbe disease. After a clinical evaluation and suspicion of Krabbe disease galactocerebrosidase activity was analyzed and *GALC* gene mutation analysis was performed. The galactocerebrosidase enzyme activity was 0.01 nmol/mg/h protein (normal range 0.8–4). For further investigation mutation screening was performed by Sanger sequencing across the 17 exons of *GALC* gene. A novel homozygous mutation c.727delT (p.S243QfsX7) was found. In this study we present the clinical findings along with a novel *GALC* mutation in a consanguineous Turkish family. Although the relationship between the various genotypes and phenotypes in Krabbe disease has not been fully elucidated an accurate genetic family study is helpful for genetic counseling follow-up and therapy of Krabbe disease. Also, it is important to identify new mutations in order to clarify their clinical importance, to assess the prognosis of the disease, and to suggest either prenatal diagnosis or preimplantation genetic diagnosis to the effected families.

1. Introduction

Krabbe disease (KD) (OMIM #245200) which is also known as globoid cell leukodystrophy is an autosomal recessive lysosomal disorder affecting the white matter of the central and peripheral nervous systems. This is a severe neurodegenerative disorder caused by deficiency of the lysosomal enzyme galactosylceramide beta-galactocerebrosidase (*GALC*) that is responsible for the degradation of certain galactolipids found in myelin (Puckett et al., 2012). The median prevalence of the disease is estimated to be approximately 1 in 100,000 births with wide variations between countries (Fiumara et al., 2011). Krabbe disease is the third among the sphingolipidoses in Turkey after metachromatic leukodystrophy and Tay–Sachs disease (Ozkara and Topçu, 2004). There are some different forms of the disease that vary in the age of onset and clinical course. The classical early infantile type is the most common disease manifestation (95% of known cases) but the disease may also present later in infancy, in childhood, or even adulthood (Fiumara et al., 2011). In the classical early infantile type of the disease symptoms usually appear before 6 months of age and with death generally before 2 years of age. Most of the patients with the infantile form of the disease present with sudden onset irritability startle response to stimuli and psychomotor regression, as well as rapid progressive motor deterioration with generalized hypertonia, hyperreflexia, spasticity, seizures, and nystagmus. Feeding difficulties and aspiration problems are frequent complications (Puckett et al., 2012; Wenger et al., 2000). Brain imaging usually shows white matter changes and/or symmetric cerebral and cerebellar demyelination, as well as changes in the basal nuclei and corpus callosum and intracranial calcifications. Generalized brain atrophy with dilatation of the ventricles and subarachnoideal spaces is evident later in the course of the disease. Peripheral nerve conduction velocities are also usually slow. Residual *GALC* enzyme activity in Krabbe patients ranges from 0 to 22% of normal values with leukocyte galactocerebrosidase levels significantly lower than the normal value (normal range 0.8–4) (Fiumara et al., 2011; Tappino et al., 2010). The *GALC* gene encodes a lysosomal protein which hydrolyzes the galactose ester bonds of galactosylceramide, galactosylsphingosine, lactosylceramide, and monogalactosyldiglyceride and mutations in this gene have been associated with KD. The gene was mapped to chromosome 14q31 (Cannizzaro et al., 1994) and contains 17 exons spanning

Abbreviations: EEG, Electroencephalogram; GALC, Galactosylceramide beta-galactocerebrosidase; HSCT, Human Stem Cell Therapy; KD, Krabbe disease; MRI, Magnetic Resonance Imaging; PCR, Polymerase Chain Reaction.

* Corresponding author. Tel.: +90 3522222246.

0378-1119/$ – see front matter © 2012 Elsevier B.V. All rights reserved.
http://dx.doi.org/10.1016/j.gene.2012.12.040

about 60 kb of genomic DNA with a GC-rich promoter region similar to the genes of other lysosomal proteins (Luzi et al., 1995). The open reading frame codes for a protein of 669 amino acids, with a molecular mass of approximately 73 kDa. To date approximately 80 distinct mutations have been identified in the *GALC* gene as the cause of KD (Sakai et al., 1994; Tappino et al., 2010).

2. Materials and methods

2.1. Clinical evaluations

A 4 month-old male child born to consanguineous parents was referred to our department with complaints of irritability, continuous crying, poor head control, hypersensitivity to auditory stimuli and generalized convulsion with occasional myoclonic episodes. The antenatal and birth history was uneventful and birth weight was 2.8 kg. His weight, height, and the head circumference were found to be in the 10th centile. At three months, he was developmentally normal. Soon thereafter, his development plateaued and rapidly regressed. Persistent vomiting began around four months of age, and increased during the last month. Physical examination revealed an alert, well nourished and very irritable infant with generalized hypertonia, increased deep tendon reflexes and arching. No organomegaly was present on examination of abdomen. Fundoscopic examination revealed that both disks were pale with bilateral nystagmus. Hearing appeared normal. Other systemic examination was normal. MRI of the brain demonstrated bilateral, symmetrical hyperintense signal changes in cerebellar dentate nuclei and deep white matter of the cerebral hemispheres (Fig. 1). EEG finding revealed bilateral sharp and slow wave discharge. Nerve conduction velocities were abnormal. He was started on phenobarbital to treat his seizures. HSCT has been considered but suitable donor was not found. By 5 months of age, the child lost all previously acquired milestones and developed severe spasticity. A gastrostomy tube was placed due to dysphagia and aspiration. He became progressively unable to manage his oral secretions and succumbed to aspiration pneumonia at 7 months of age (Table 1). This study was approved by Erciyes University Ethics Committee and signed informed consent was obtained from the family.

Table 1
Phenotypic characteristics of the patient.

Gender	Male
Consanguity of the parents	+
Age at onset	3 months
Cerebral cry	+
Regression	+
Fever	−
Febrile seizures	−
Hypotonia	+
Irritability	+
Hemiplegia/diplegia	+
Nystagmus	+
Optic atrophy	Both disks were pale
Behavioral signs	+
Tremors	−
Deterioration	+
Tetraplegia	+
Hypertonia, Hyperreflexia	+
Clonus	−
Peripheral neuropathy	+
Seizures	+
Hypersensitivity to auditory stimuli	+
Dysarthria	−
Dysphagia	+
Age at death	5 months old
Neuroradiologic findings	+
Abnormal nerve conduction velocity	+

2.2. Method

After clinical evaluation and suspicion of KD leukocyte galactocerebrosidase activity was measured using the radiolabeled natural substrate galactosylceramide and compared with the laboratory's reference ranges. *GALC* gene mutational analysis was performed. Genomic DNA from the proband and the parents was extracted from peripheral blood by a conventional phenol–chloroform method. The 17 exons of *GALC* gene were PCR amplified using primers described by Xu et al. (2006). Amplified fragments were purified by Suprec PCR kit (Takara) as per manufacturer's guideline. Products were directly sequenced following purification and cycle sequencing reactions.

3. Results

The galactocerebrosidase enzyme activity of the patient was found to be 0.01 μmol/g/h (normal range 0.8–4). Sequencing of the *GALC* exome revealed a novel homozygous mutation c.727delT (p.S243QfsX7) and both parents were heterozygous for this mutation (Fig. 2).

4. Discussion

The galactosylceramidase (*GALC*) gene is located on 14q31. To date at least 80 *GALC* mutations have been identified that cause KD (Wenger et al., 2000). The most frequent mutation (>35% of KD patients in most European countries and in USA) is a large (30-kb) deletion (Wenger et al., 2000). In a study sixty-four unrelated patients with infantile Krabbe disease of Dutch or other European origin were screened for the presence of a large 30 kb deletion starting in intron 10 (IVS10del30kb). The deletion was also found in a patient from Turkey (Kleijer et al., 1997). To the best of our knowledge this

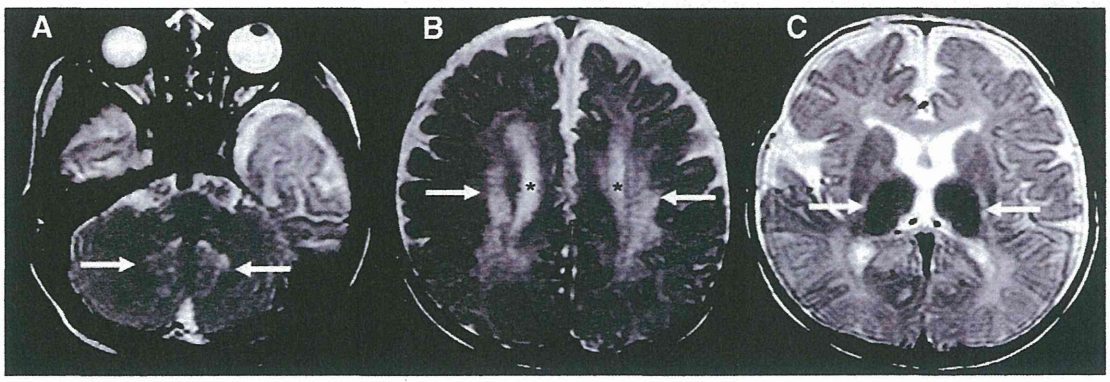

Fig. 1. Axial T2-weighted TSE images through the level of cerebellum (A) and upper lateral ventricles (t) (B) show bilateral, symmetrical hyperintense signal changes in cerebellar dentate nuclei (arrows) (A), and deep white matter of the cerebral hemispheres (arrows) (B). The thalami are diffuse hypointense on T2-weighted TSE images which is a characteristic finding of Krabbe disease (arrows) (C).

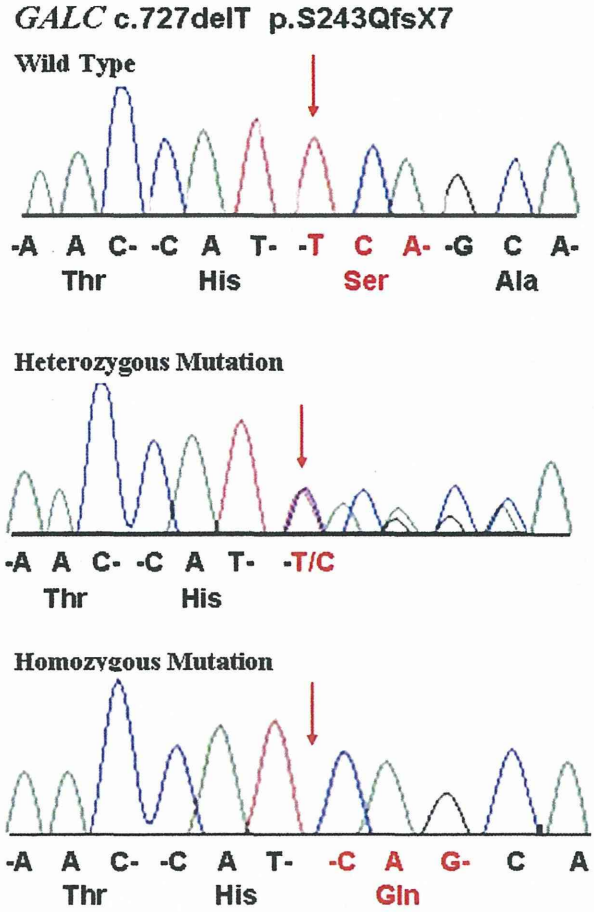

Fig. 2. DNA sequencing of the patient showed a novel homozygous mutation c.727delT resulting in p. S243QfsX in *GALC* gene. Both parents were heterozygous for this mutation.

was the first report regarding the molecular genetic determination of a KD patient from Turkey. p.T513M and p.Y551S are also frequent mutations found in infant KD patients, whilst p.G270D is common among adult-onset patients (Wenger et al., 2000). The c.121G>A mutation has been shown with longer survival in a selected population with high rate of late onset forms (Fiumara et al., 2011). Some common polymorphisms (especially c.1637G>C and c.502C>T) influence enzyme activity and may be responsible for a pseudodeficiency state, particularly when in compound heterozygosity with a disease-causing allele (Wenger et al., 2000). The novel mutation c.727delT (p.S243QfsX7) found in this study is a single base-pair deletion in codon 242 which causes a frame shift mutation, resulting in premature termination of the *GALC* protein at codon 249. This sequence motif is thought to play a critical role in the targeting of proteins and it is therefore unlikely that this truncated mutant protein was functional.

In this case, the onset of the disease was very early and disease progression was very rapid. The time of onset of the symptoms was similar to patients with other mutations resulting in early-onset forms of the disease but progression of the symptoms in this patient was much quicker than other reported forms of KD (Duffner et al., 2011). In a study of Duffner et al. (2011) in 112 patients with Krabbe disease, the most common symptoms at presentation were; crying-irritability (49%), fisted hands (33%), poor head control (28%), and poor feeding (24%). Our patient was admitted to our clinic with the complaints of irritability, crying and poor head control. The mean survival of KD patients is between 13 and 25 months depending on the study (Duffner et al., 2011). Although very low galactocerebrosidase activity was not associated with the survey (Duffner et al., 2011) our patient's enzyme activity was very low and the survey was very short. But we think that, one patient is not enough for the evaluation for enzyme–survey association. EEG of the patient was abnormal. Husain et al. reported EEG results in 14 symptomatic children, and 79% were abnormal (Husain et al., 2004). Nerve conduction velocity was abnormal as in other studies in symptomatic children with early infantile KD (Husain et al., 2004; Siddiqi et al., 2006). Newborn screening has been performed for KD (Duffner et al., 2011). Screening involves *GALC* activity detection by a fluorescent assay and subsequent DNA mutation analysis. Molecular analysis of the *GALC* gene is used for diagnostic confirmation. Human Stem Cell Therapy (HSCT) is the only available treatment for infants with early infantile KD and must be performed prior to neurodegeneration. Newborns treated with HSCT can have progressive central myelination and continued gains in developmental skills and cognitive function, whereas children who undergo transplantation after onset of symptoms experience minimal neurologic improvement. Transplantation is not effective in all cases of KD and some transplanted patients have experienced developmental delays (Siddiqi et al., 2006). As a result in this study we present the clinical findings along with a novel *GALC* mutation in a consanguineous Turkish family. Although the genotype–phenotype relationship has not been fully elucidated in KD, an accurate genetic family study is helpful for genetic counseling, the follow-up and therapy of KD patients. Also, it is important to identify new mutations in order to clarify their clinical importance, to assess the prognosis of the disease, and to suggest prenatal diagnosis or preimplantation genetic diagnosis to the affected families.

References

Cannizzaro, L.A., et al., 1994. Regional mapping of the human galactocerebrosidase gene (GALC) to14q31 by in situ hybridization. Cytogenet. Cell. Genet. 66, 244–245.
Duffner, P.K., et al., 2011. Early infantile Krabbe disease: results of the world-wide Krabbe registry. Pediatr. Neurol. 45, 141–148.
Fiumara, A., et al., 2011. Krabbe leukodystrophy in a selected population with high rate of late onset forms: longer survival linked to c.121G>A (p.Gly41Ser) mutation. Clin. Genet. 80, 452–458.
Husain, A.M., et al., 2004. Krabbe disease: neurophysiologic studies and MRI correlations. Neurology 63, 617–620.
Kleijer, W.J., et al., 1997. Prevalent mutations in the GALC gene of patients with Krabbe disease of Dutch and other European origin. J. Inherit. Metab. Dis. 20, 587–594.
Luzi, P., et al., 1995. Structure and organization of the human galactocerebrosidase (GALC) gene. Genomics 26, 407–409.
Ozkara, H.A., Topçu, M., 2004. Sphingolipidoses in Turkey. Brain Dev. 26, 363–366.
Puckett, R.L., et al., 2012. Krabbe disease: clinical, biochemical and molecular information on six new patients and successful retrospective diagnosis using stored newborn screening cards. Mol. Genet. Metab. 105, 126–131.
Sakai, N., et al., 1994. Krabbe disease: isolation and characterization of a full-length cDNA for human galactocerebrosidase. Biochem. Biophys. Res. Commun. 198, 485–491.
Siddiqi, Z.A., et al., 2006. Peripheral neuropathy in Krabbe disease: electrodiagnostic findings. Neurology 67, 263–267.
Tappino, B., et al., 2010. Identification and characterization of 15 novel GALC gene mutations causing Krabbe disease. Hum. Mutat. 31, 1894–1914.
Wenger, D.A., et al., 2000. Krabbe disease: genetic aspects and progress toward therapy. Mol. Genet. Metab. 70, 1–9.
Xu, C., et al., 2006. Six novel mutations detected in the GALC gene in 17 Japanese patients with Krabbe disease, and new genotype–phenotype correlation. J. Hum. Genet. 51, 548–554.

RESEARCH ARTICLE

AMERICAN JOURNAL OF medical genetics PART A

Microdeletions of 3p21.31 Characterized by Developmental Delay, Distinctive Features, Elevated Serum Creatine Kinase Levels, and White Matter Involvement

Kaoru Eto,[1] Norio Sakai,[2] Shino Shimada,[1,3] Mutsuki Shioda,[1] Keiko Ishigaki,[1] Yusuke Hamada,[2] Michiko Shinpo,[2] Junji Azuma,[2] Koji Tominaga,[2] Keiko Shimojima,[3] Keiichi Ozono,[2] Makiko Osawa,[1] and Toshiyuki Yamamoto[3]*

[1]Department of Pediatrics, Tokyo Women's Medical University, Tokyo, Japan

[2]Department of Pediatrics, Osaka University Graduate School of Medicine, Suita, Japan

[3]Tokyo Women's Medical University Institute for Integrated Medical Sciences, Tokyo, Japan

Manuscript Received: 24 February 2013; Manuscript Accepted: 27 June 2013

Interstitial deletions of chromosome 3 are rare, and only one patient with a microdeletion of 3p21.31 has been reported to date. We identified two additional cases of patients with microdeletions of 3p21.31. The characteristic clinical features of developmental delay and distinctive facial features (including arched eyebrows, hypertelorism, epicanthus, and micrognathia) were seen both in the previously reported patient and in the two newly identified patients. In these two new cases, additional features, including elevated serum creatine kinase levels and characteristic neuroradiological features with white matter involvement, were seen. These features had not been described in the previous case in which the patient was examined during infancy, suggesting an age-dependent mechanism. The shortest region of overlap among the three deletions narrowed down the candidate genes that may be responsible for the common neurological features to the bassoon (presynaptic cytomatrix protein) gene (*BSN*), which has an important function in neuronal synapses. In this study, we confirmed common phenotypic features in the patients with microdeletions of 3p21.31 and identified additional features that have not been reported previously. Because the constellation of such characteristic features is quite unique, clinical manifestations of the patients with microdeletions of 3p21.31 would be clinically recognizable as a contiguous gene deletion syndrome.

Key words: microdeletion of 3p21.31; developmental delay; distinctive facial features; white matter involvement; the bassoon (presynaptic cytomatrix protein) gene (*BSN*); elevated serum creatine kinase (CK)

How to Cite this Article:
Eto K, Sakai N, Shimada S, Shioda M, Ishigaki K, Hamada Y, Shinpo M, Azuma J, Tominaga K, Shimojima K, Ozono K, Osawa M, Yamamoto T. 2013. Microdeletions of 3p21.31 characterized by developmental delay, distinctive features, elevated serum creatine kinase levels, and white matter involvement.
Am J Med Genet Part A 161A:3049–3056.

INTRODUCTION

Many of the newly identified chromosomal microdeletion syndromes have been established following the spread of chromosomal microarray testing throughout the world [Slavotinek, 2008]. Some of the newly established chromosomal microdeletion syndromes resulting from interstitial chromosomal microdeletions are caused by non-allelic homologous recombination (NAHR) mechanisms mediated by two neighboring low-copy repeats; for example, 16p11.2 deletion/duplication and 17q21.31 deletion [Koolen et al., 2008; Shinawi et al., 2010]. Patients with identical chromosomal microdeletion syndromes show the same clinical features because of the fact that the deletion size is exactly the same among

Conflict of interest: none.
Grant sponsor: Ministry of Education, Culture, Sports, Science and Technology (MEXT); Grant sponsor: Ministry of Health, Labor, and Welfare, Japan.
*Correspondence to:
Dr. Toshiyuki Yamamoto, Tokyo Women's Medical University Institute for Integrated Medical Sciences, Kawada-cho 8-1, Shinjuku-ward, Tokyo 162-8666, Japan.
E-mail: yamamoto.toshiyuki@twmu.ac.jp
Article first published online in Wiley Online Library (wileyonlinelibrary.com): 16 August 2013
DOI 10.1002/ajmg.a.36156